Effect of Retardation on Crack Propagation Life Distribution under Random Loading

Effect of Retardation on Crack Propagation Life Distribution under Random Loading

Hidetoshi ISHIKAWA*, Hiroshi ISHIKAWA** and Yoshisada MUROTSU***

(Received November 15, 1990)

The present paper deals with program development for the simulation of the effect of retardation on the fatigue crack propagation life distribution under random loading in reference to the fact that the correct prediction of fatigue life or fatigue strength becomes of crucial importance since almost all practical machines and structures are usually subjected to random loading, and most of their failures are caused by fatigue. In this respect, first, a simulation program in consideration of the effect of retardation caused by overload is developed to predict fatigue life under random loading with the aid of experimental data obtained comparatively easily by constant amplitude fatigue tests. This simulation program is expected to provide a quite effective measure for the reliability analysis of fatigue life with wide applicability. Then, by use of the program, the effect of retardation is investigated. In case of ignoring the retardation effect, fatigue life is naturally estimated to be shorter. On the other hand, in consideration of the retardation effect, the Willenborg model brings more risky results such that the life becomes longer than that based on the Vroman model. Therefore, the Vroman model may be considered more rational than the Willenborg model in a practical sense.

1. Introduction

Structural reliability assurance is of vital importance in designing structures of much societal concern such as airplanes, bridges and buildings, since their fracture will cause, directly or indirectly, a fatal loss of human life. The failure of these structures is mostly due to fatigue caused by randomly applied external stresses. Cracks are initiated in structural components due to the repetition of random loading and they grow gradually until final failures take place. Therefore, in the reliability-based fatigue-proof design, the correct prediction of fatigue life and

* Department of Information Systems, Kagawa College of Technology, Marugame, Kagawa, Japan

** Department of Information Science, Kagawa University, Takamatsu, Kagawa, Japan

*** Department of Aeronautical Engineering, University of Osaka Prefecture, Sakai, Osaka, Japan

fatigue strength of structural components becomes indispensable. For this purpose, a so-called full scale fatigue test is considered most desirable under service conditions. This kind of fatigue test, however, requires large amount of cost with respect to time, labor and/or expenses.

In reference to the above, the present study first deals with the construction of fatigue crack growth model on a structural component subjected to random loading in consideration of the retardation effect due to overloads which exceed the yield strength of the material used, based upon the recent remarkable advance of fracture mechanics. Then, this paper devotes itself to the program development for the simulation of fatigue life under random loading by use of some parameter values which are obtained easily by the test of constant stress amplitude. Finally, the effect of retardation on the crack propagation life distribution is exemplified with the aid of the program thus developed.

2. Technical Background of Fracture Mechanics for Fatigue Crack Growth Law

2.1 Fatigue crack growth law

In general, the fatigue crack growth law can be expressed in the following form:

$$\frac{da}{dn}=f(a,\ \sigma_{max},\ R,\ T,\ E,\cdots) \tag{1}$$

where

a = the crack length after n cycles of stressing,
da/dn = the crack growth rate after n cycles of stressing,
σ_{max} = the maximum stress level at the n-th cycle,
σ_{min} = the minimum stress level at the n-th cycle,
$R=\sigma_{min}/\sigma_{max}$ = the stress ratio at the n-th cycle,
T = temperature, and
E = other environmental conditions.

Based upon Eq.(1), various studies on the crack growth law have been recently made and a variety of the following crack growth laws have been constructed and proposed:

(a) Paris-Erdogan's growth law

Recent advancement in fracture mechanics has shown that the crack growth rate can be expressed in terms of the stress intensity factor range ΔK at the crack tip defined as

$$\Delta K=K_{max}-K_{min}=(1-R)K_{max} \tag{2}$$

where

$$K_{max} = \sigma_{max}\sqrt{\pi a} \quad \text{=the maximum stress intensity factor} \tag{3-a}$$

$$K_{min} = \sigma_{min}\sqrt{\pi a} \quad \text{=the minimum stress intensity factor} \tag{3-b}$$

for through-the-thickness cracks when the correction factor due to the finite specimen size is disregarded.

Paris proposed the 4th power type growth law based upon the experimental results on aluminum alloy in the following form[1]:

$$\frac{da}{dn} = f(\Delta K) = C(\Delta K)^4 \tag{4}$$

where C is a material constant.

At present, the Paris' cack growth law is widely applied in the following generalized form which is often termed as the Paris-Erdogan's growth law:

$$\frac{da}{dn} = C(\Delta K)^m \tag{5}$$

where C and m are material constants. This equation indicates that the crack growth rate is primarily determined by ΔK and the effects of the stress ratio, the repetition speed of stressing and the specimen thickness would be regarded as secondary, being reflected in the material constants such as C and m. Though the value of the exponent m practically assumes 2~8 according to the material, it is often the case for fatigue life estimation that m is approximated by 4 as the representative value which Paris first proposed. Taking the natural logarithm of

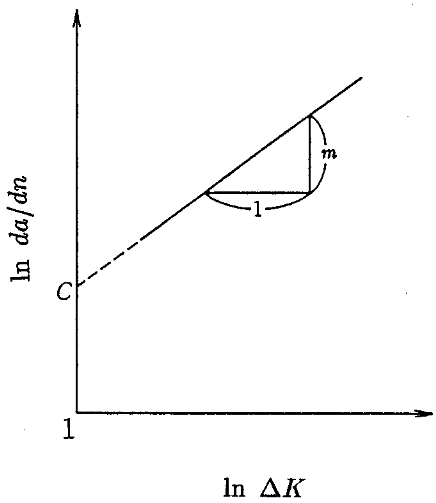

Fig. 1 The linear relationship between da/dn and ΔK.

both sides of Eq.(5), it follows that

$$\ln\left(\frac{da}{dn}\right)=\ln C+m\ln(\Delta K) \tag{6}$$

From this equation, as shown in Fig. 1, the relationship between da/dn and ΔK becomes linear if both quantities are measured on a logarithmic scale. As can be easily seen, the exponent m represents the slope of this straight line and C the value of the ordinate for $\Delta K=1$.

(b) Forman, *et al.*'s equation

In reference to the fact that the crack growth rate increases quite rapidly, widely apart from the straight line of the Paris-Erdogan's law, when the value of the maximum stress intensity factor K_{max} approaches that of the fracture toughness K_{IC}, the following equation of crack growth law is proposed by Forman, *et al.*[2].

$$\frac{da}{dn}=\frac{C(\Delta K)^m}{(1-R)K_{IC}-\Delta K}=\frac{C(\Delta K)^m}{(1-R)(K_{IC}-K_{max})} \tag{7}$$

where the constant value C and the exponent m are similar to those of the Paris-Erdogan's law, but not necessarily the same, and $R=\sigma_{min}/\sigma_{max}$ represents the stress ratio.

(c) Collipriest's equation

A progress in the research on the relationship between da/dn and ΔK has clarified that $\ln(da/dn)-\ln(\Delta K)$ curve has a sigmoidal shape, as shown in Fig. 2, between the fracture toughness K_{IC} and the threshold stress intensity factor range ΔK_{th}. From

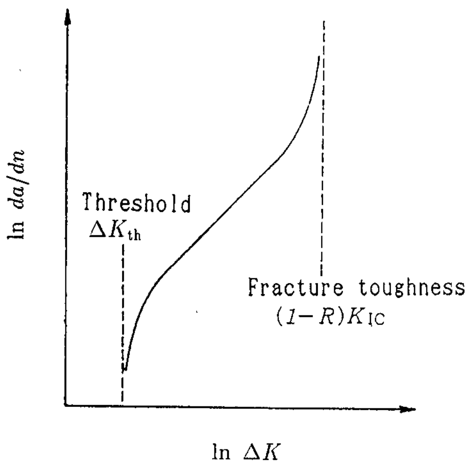

Fig. 2 The relationship between $\ln(da/dn)$ and $\ln(\Delta K)$ showing a sigmoidal shape.

this point of view, Collipriest proposed the equation in the following form[3].

$$\frac{da}{dn}=\exp\Bigg[m\left(\frac{\ln K_{IC}-\ln\Delta K_{th}}{2}\right) \times\tanh^{-1}\left\{\frac{\ln\Delta K-\dfrac{\ln\{(1-R)K_{IC}\}+\ln\Delta K_{th}}{2}}{\dfrac{\ln\{(1-R)K_{IC}\}-\ln\Delta K_{th}}{2}}\right\} +\ln\left\{C\exp\left(\frac{\ln K_{IC}+\ln\Delta K_{th}}{2}\times m\right)\right\}\Bigg] \tag{8}$$

where m and C are material constants. The above Collipriest's equation is also termed as "sigmoidal equation".

(d) Walker's equation

The accumulation of data base of fatigue test results under constant stress amplitude has made it clear that the fatigue crack growth rate is affected also by the stress ratio R. From this viewpoint, Walker introduced the notion of effective stress range, ΔK_{eff}, which can be represented by use of the stress intensity factor as follows[4]:

$$\Delta K_{eff}=(1-R)^{v}K_{max} \tag{9}$$

where v is a material constant. Applying Eq.(9) to the generalized Paris-Erdogan's law in Eq.(5), we get

$$\frac{da}{dn}=C(\Delta K_{eff})^{m}=C[(1-R)^{v}K_{max}]^{m} \tag{10}$$

Moreover, this equation can be transformed with the aid of ΔK in Eq.(2) in the following form:

$$\frac{da}{dn}=C\left[\frac{\Delta K}{(1-R)^{1-v}}\right]^{m} \tag{11}$$

This equation is called the Walker's crack growth law, which reduces to the following equation in case of $v=1$:

$$\frac{da}{dn}=C(\Delta K)^{m}$$

This is nothing but the Paris-Erdogan's growth law as in Eq.(5).

(e) Hall, *et al.*'s equation

Hall, *et al.* proposed an experimental equation to be fitted to the crack growth data in USAF (United States Air Force) as follows[5]:

$$\frac{da}{dn}=C(K_{max}-K_{th})^{\alpha}(\Delta K)^{m} \tag{12}$$

where C, α and m are material constants obtained through the curve-fitting technique. The above equation is also called the "Boeing equation".

(f) Bell, *et al.*'s equation

Under random loading, it is often the case that overloads are imposed, which might cause retardation of the crack growth. Bell, *et al.* proposed the following equation in consideration of the preceding retardation effect[6].

$$\frac{da}{dn}=C[(1+q\bar{R})\Delta K]^{m} \tag{13}$$

where $\bar{R}$ is defined as

$$\begin{cases} \bar{R}=R & \text{for } R\leqq R_{cut} \\ \bar{R}=R_{cut} & \text{for } R>R_{cut} \end{cases} \tag{14}$$

in which R_{cut}, the cut-off stress ratio, is defined as the upper cut-off value of the stress ratio R. C, q and m are experimental constants of the material obtained through the curve-fitting technique.

It should be noted here that the above equation is derived by modifying the Elber's closure model[7] defined in the following form and is considered to give a good fit to the experimental data.

$$\begin{cases} \Delta K_{eff}=U\Delta K=\left(\dfrac{\sigma_{max}-\sigma_{op}}{\sigma_{max}-\sigma_{min}}\right)\Delta K \\ \quad U=0.5+0.4R \quad (\text{for } -0.1<R<0.7) \\ \qquad\qquad (\text{in case of 2024}-\text{T3 aluminum alloy}) \\ \quad R=\sigma_{min}/\sigma_{max} \\ \quad \sigma_{op}=\text{the crack opening stress} \end{cases} \tag{15}$$

2.2 Retardation model

Among several models proposed so far to take into consideration the above-mentioned retardation effect on the crack growth rate caused by overload, the present paper describes two well-known models, the Willenborg's model and the Vroman's model.

(a) Willenborg's model

It is the Willenborg's model[8] the purpose of which is to omit the troublesome data fitting operations required, for instance, for the model proposed by Wheeler[9]. In this model, the following assumptions are adopted:

(i) Retardation is a function of the maximum stress in each cycle of stressing and the overload immediately before it stressing.

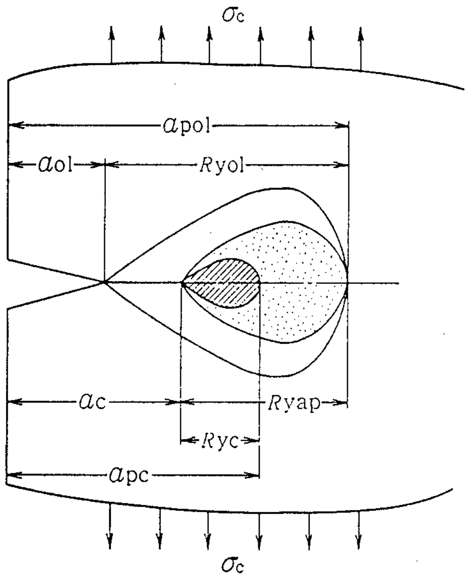

Fig. 3 Schematic representation of the plastic zone at the crack tip.

(ii) Retardation is proportional to the amount of reduction in the maximum stress by that of the residual stress due to the overload.
(iii) Retardation effect gradually decreases through the plastic zone around the crack tip caused by the overload.
(iv) In the case where a larger amount of overload is newly applied than that of the last one, a new conditional equation of retardation is formed, entirely independent of all the past conditions.
(v) Every applied stress is non-negative.

As shown in Fig. 3, assumed that the application of the overload σ_{ol} is completed at the time of the crack length a_{ol}, the size R_{yol} of the plastic zone at the crack tip is given, by Irwin, as follows:

$$R_{yol}=\frac{1}{c\pi}\left(\frac{K_{maxol}}{\sigma_y}\right)^2 \tag{16}$$

where

$$\left.\begin{aligned} K_{maxol}&=\text{the maximum stress intensity factor caused by the overload } \sigma_{ol}\\ \sigma_y&=\text{the yield stress of the material}\\ c&=2 \quad \text{(in case of plain stress condition)}\\ &=4\sqrt{2}\ \text{(in case of plain strain condition)} \end{aligned}\right\} \tag{17}$$

Therefore, the zone size a_{pol} affected by the overload σ_{ol} is

$$a_{pol}=a_{ol}+R_{yol} \tag{18}$$

Suppose that σ_c is the applied stress at the crack length $a=a_c(<a_{pol})$. Then K_{max}, the

stress intensity factor at that time, and the plastic zone size at the crack tip for $\sigma=\sigma_c$ are given, respectively, as

$$K_{max}=\sigma_c\sqrt{\pi a_c} \tag{19}$$

$$R_{yc}=\frac{1}{c\pi}\left(\frac{K_{max}}{\sigma_y}\right)^2 \tag{20}$$

Hence, the total size a_{pc} of the zone affected by σ_c can be expressed as

$$a_{pc}=a_c+R_{yc} \tag{21}$$

With the aid of Eqs.(18) and (21), the conditional equation of the retardation can be constructed in the following way:

(i) If $a_{pc}>a_{pol}$, through the assumption, a new conditional equation of the retardation is constructed. Therefore, the quantities

$$\begin{cases} a_{pol}\leftarrow a_{pc} \\ R_{yol}\leftarrow R_{yc} \\ K_{maxol}\leftarrow K_{max} \end{cases}$$

are replaced, as shown in the above, by the new ones, respectively.

(ii) If $a_{pc}\leqq a_{pol}$, the crack growth is retarded. This retardation effect is due to the residual stress calculated in the following fashion. That is, the stress intensity factor K_{maxap}, which satisfies Eq.(23), corresponding to the apparent stress σ_{ap} which would produce the same size of plastic zone as the residual size R_{yap} of the plastic zone at the present is first computed as follows:

$$R_{yap}=a_{pol}-a_c \tag{22}$$

$$R_{yap}=\frac{1}{c\pi}\left(\frac{K_{maxap}}{\sigma_y}\right)^2 \tag{23}$$

$$K_{maxap}=\sigma_{ap}\sqrt{\pi R_{yap}} \tag{24}$$

With the aid of σ_{ap}, thus obtained the residual stress

$$\sigma_{res}=\sigma_{ap}-(\sigma_c)_{max} \tag{25}$$

is calculated, and then, the stress intensity factor

$$K_{res}=K_{maxap}-K_{max} \tag{26}$$

is obtained. The retardation caused by this residual stress can be evaluated by re-calculating $(K_{max})'$, $(K_{min})'$ and R' as follows:

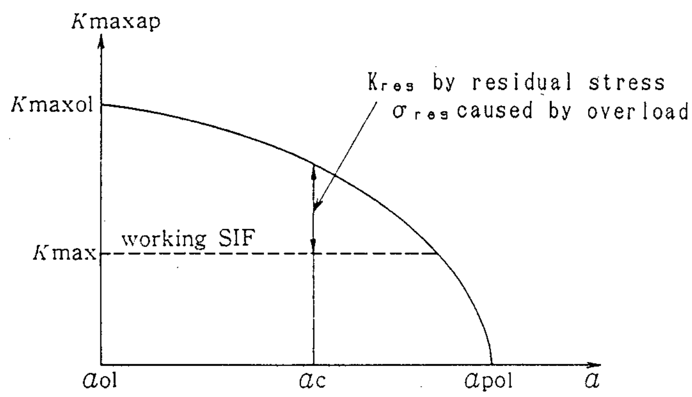

Fig. 4 The residual stress caused by retardation.

$$\left.\begin{aligned}(K_{max})' &= K_{max} - K_{res}\\ &= 2K_{max} - K_{maxap}\\ (K_{min})' &= K_{min} - K_{res}\\ &= (K_{max} + K_{min}) - K_{maxap}\\ R' &= (K_{min})'/(K_{max})'\end{aligned}\right\} \tag{27}$$

Figure 4 represents the relationship between Eqs.(23) and (26). By the way, it follows through Eqs.(16), (18) and (23) that

$$(K_{maxap})^2 = c\pi\sigma_y^2(a_{pol} - a_c)$$

Therefore, we have the following relationships:

$$\begin{aligned}K_{maxap} &= K_{maxol}\sqrt{\frac{a_{pol} - a_c}{R_{yol}}}\\ &= K_{maxol}\sqrt{\frac{a_{pol} - a_c}{a_{pol} - a_{ol}}}\end{aligned} \tag{28}$$

$$a_c = a_{pol} - (a_{pol} - a_{ol})\left(\frac{K_{maxap}}{K_{maxol}}\right)^2 \tag{29}$$

The retardation effect based upon the Willenborg's model can be evaluated by use of Eq.(27). Since this model treats only non-negative stresses, negative stresses need to be replaced by 0 and, in addition, $K_{maxap} = K_{maxol}$ holds through Eq.(28), since $a_c = a_{ol}$ holds immediately after the loading of the overload σ_{ol}. Therefore, the following three modes of retardation effects can be categorized according to which is larger or smaller between the overload σ_{ol} and the successively applied stress σ_c.

(i) Mode I

This is the retardation mode based upon the reduction both of ΔK and R. This mode corresponds to the case that $(K_{max})' > 0$ and $(K_{min})' \leqq 0$. Therefore,

$$\left.\begin{array}{l} K_{min}+K_{max}\leqq K_{maxol}<2K_{max} \\ (\sigma_c)_{min}+(\sigma_c)_{max}\leqq \sigma_{ol}<2(\sigma_c)_{max} \end{array}\right\} \tag{30-a}$$

In this case, since equations hold such that $(K_{max})_{eff}=(K_{max})'$ and $(K_{min})_{eff}=0$, it follows that

$$\left.\begin{array}{l} \Delta K_{eff}=(K_{max})'=K_{max}-K_{res} \\ R_{eff}=(K_{min})_{eff}/(K_{max})_{eff}=0 \end{array}\right\} \tag{30-b}$$

(ii) Model II

This is the retardation mode based upon the reduction only of R. This mode corresponds to the case that $(K_{min})'>0$. Therefore,

$$\left.\begin{array}{l} K_{min}+K_{max}>K_{maxol} \\ (\sigma_c)_{min}+(\sigma_c)_{max}>\sigma_{ol} \end{array}\right\} \tag{31-a}$$

In this case, since equations hold such that $(K_{max})_{eff}=(K_{max})'$ and $(K_{min})_{eff}=(K_{min})'$, it follows that

$$\left.\begin{array}{rl} \Delta K_{eff} &=(K_{max})_{eff}-(K_{min})_{eff} \\ &=K_{max}-K_{min}=\Delta K \\ R_{eff} &=(K_{min})_{eff}/(K_{max})_{eff} \\ &=(K_{min}-K_{res})/(K_{max}-K_{res}) \end{array}\right\} \tag{31-b}$$

(iii) Mode III

This is the mode where maximum retardation is produced. In this mode, the crack growth ceases completely and this corresponds to the case that $(K_{max})'\leqq 0$. Therefore,

$$\left.\begin{array}{l} 2K_{max}\leqq K_{maxol} \\ 2(\sigma_c)_{max}\leqq \sigma_{ol} \end{array}\right\} \tag{32-a}$$

In this case, since the equation that $(K_{max})_{eff}=(K_{min})_{eff}=0$ holds, it follows that

$$\left.\begin{array}{l} \Delta K_{eff}=0 \\ R_{eff}=0 \end{array}\right\} \tag{32-b}$$

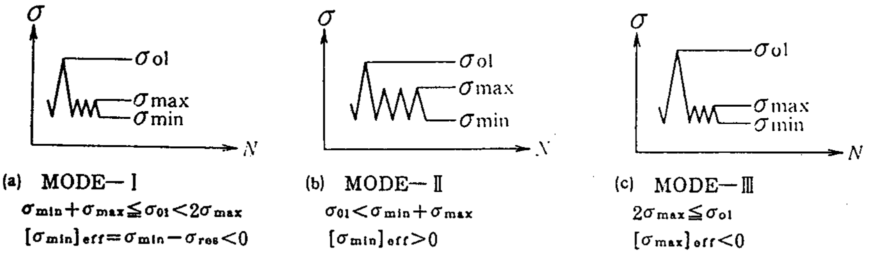

(a) MODE—I
$\sigma_{min}+\sigma_{max}\leqq\sigma_{01}<2\sigma_{max}$
$[\sigma_{min}]_{eff}=\sigma_{min}-\sigma_{res}<0$
$\therefore\ [\sigma_{min}]_{eff}=0$
$[\Delta K]_{eff}=[K_{max}]_{eff}$
$[R]_{eff}=0$

(b) MODE—II
$\sigma_{01}<\sigma_{min}+\sigma_{max}$
$[\sigma_{min}]_{eff}>0$
$\therefore\ [\Delta K]_{eff}=[\Delta K]$
$[R]_{eff}=\dfrac{[K_{min}]_{eff}}{[K_{max}]_{eff}}$

(c) MODE—III
$2\sigma_{max}\leqq\sigma_{01}$
$[\sigma_{max}]_{eff}<0$
$[\sigma_{min}]_{eff}<0$
$\therefore\ [\sigma_{max}]_{eff}=[\sigma_{min}]_{eff}=0$
$[\Delta K]_{eff}=[R]_{eff}=0$

Fig. 5 Willenborg's retardation model.

The applied stress condition is schematically represented in Fig. 5 corresponding to the abovestated modes I~III. By the way, σ_{o1}/σ_c is termed as the overload ratio. In the Willenborg's model, the crack growth is predicted to cease when this ratio becomes more than or equal to 2. In fact, the cease of crack growth is reported in case of $\sigma_{o1}/\sigma_c \geqq 2.3$ in aluminum alloy[10].

The crack growth can be predicted by applying ΔK_{eff} and R_{eff} obtained based upon the above method to any of the preceding crack growth laws, for example, the Paris-Erdogan's law or the Walker's law.

(b) Vroman's model[11]

Though this model is similar to the preceding Willenborg's model, the way to calculate ΔK_{eff} and R_{eff} is different, respectively. This model utilizes the stress ratio $R=\sigma_{min}/\sigma_{max}$ as it is for R_{eff} and uses the following equation for ΔK_{eff}.

$$\left.\begin{aligned} R_{eff} &= R = K_{min}/K_{max} && \text{for } R \leqq R_{cut} \\ &= R_{cut} && \text{for } R > R_{cut} \end{aligned}\right\} \tag{33}$$

$$\Delta K_{eff} = (K_{max} - K_{min}) - \frac{1}{3}\left[K_{maxo1}\sqrt{\frac{a_{o1}+R_{yo1}-a_c}{R_{yo1}}} - K_{max} \right] \tag{34}$$

where

$$R_{yo1} = \frac{1}{c\pi}\left(\frac{K_{maxo1}}{\sigma_y}\right)^2$$

σ_y = the yield stress of the material

K_{max} = the maximum stress intensity factor under the current loading cycle

K_{min} = the minimum stress intensity factor under the current loading cycle

$$\left.\begin{matrix} a_{o1} \\ R_{yo1} \\ K_{maxo1} \end{matrix}\right\} \text{ values based on the overload } \sigma_{o1} \text{ previously loaded}$$

It is a standard practice to apply ΔK_{eff} and R_{eff} defined by the aforementioned method to a certain suitable crack growth law. For example, in applying to the Walker's law, the equation becomes as follows:

$$\frac{da}{dn} = C\left[\frac{\Delta K_{eff}}{(1-R_{eff})^{1-v}}\right]^m \tag{35}$$

where C, m and v are material constants to be obtained by experimental data under the constant stress amplitude test.

2.3 Equation of stress intensity factor

A variety of calculations for the stress intensity factor K are made in detail according to various combinations between shapes of specimens and stress conditions[12,13]. The present paper deals with the uniform tension of plain plate both with through-the-thickness center crack and with through-the-thickness single edge

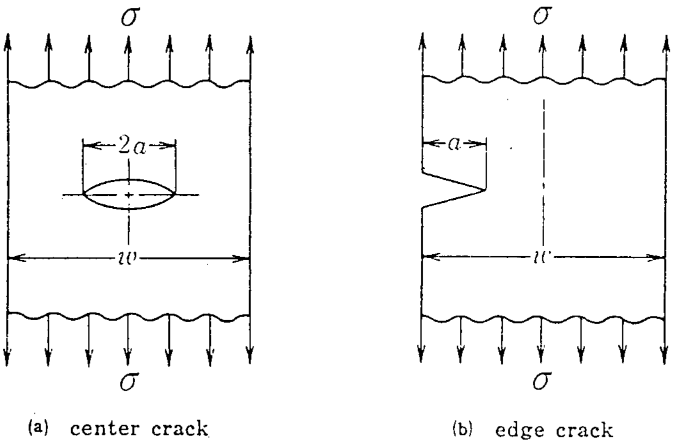

Fig. 6 Through-the-thickness center crack and single edge crack.

crack, as shown in Fig. 6.

(i) Uniform tension of plain plate with through-the-thickness center crack

In this case, the stress intensity factor K corresponding to the applied stress σ is approximated in the following form:

$$\left.\begin{aligned} K &= \sigma\sqrt{\pi a}F\left(\frac{2a}{w}\right) \\ \xi &= 2a/w \\ F(\xi) &\cong \sqrt{\sec\left(\frac{\pi\xi}{2}\right)} \end{aligned}\right\} \tag{36}$$

where $F(\xi)$ is a correction factor associated with specimen geometries. Approximation error is 0.3% for $\xi \leqq 0.7$, and 1% for $\xi = 0.8$.

(ii) Uniform tension of plain plate with through-the-thickness single edge crack

The stress intensity factor K for the applied stress σ can be approximated as follows:

$$\left.\begin{aligned} K &= \sigma\sqrt{\pi a}F\left(\frac{a}{w}\right) \\ \xi &= a/w \\ F(\xi) &\cong 1.12 - 0.231\xi + 10.55\xi^2 - 21.72\xi^3 + 30.39\xi^4 \end{aligned}\right\} \tag{37}$$

Approximation error is 0.5% for $\xi \leqq 0.6$.

3. Program Development for Simulation of Fatigue Crack Growth in Consideration of Retardation

3.1. Crack growth law applied in the program

Among various crack growth laws stated earlier, the most essential and popular laws could be pointed out as follows:

(i) Paris-Erdogan's law
(ii) Forman's law, and
(iii) Walker's law

The Paris-Erdogan's law is utilized most often for its ease of use. Though the Forman's law is considered to be characteristic in consideration of the effect of K_{IC}, the Walker's law would be adopted more often for researcher's liking.

Consequently, in developing the simulation program for the prediction of fatigue crack growth under random loading in the present study, the following two types of crack growth laws are adopted:

(i) Paris-Erdogan's law

$$\frac{da}{dn}=C(\Delta K)^m \tag{38}$$

(ii) Walker's law

$$\frac{da}{dn}=C\left[\frac{\Delta K}{(1-R)^{1-v}}\right]^m \tag{39}$$

The program is made so as to be able to choose either law properly, as the occasion may demand, by use of the control parameter NTYPE in the following fashion:

NTYPE$=0$ → The Paris-Erdogan's law is chosen.
NTYPE$\neq 0$ → The Waker's law is selected.

3.2. Retardation model applied in the program

The Willenborg or the Vroman model can be selected properly according to the practical necessity through the control parameter NRETRD. Such a case of disregarding the effect of the retardation is also involved as follows:

NRETRD$\leqq 0$ →This corresponds to the case of neglecting the retardation effect.
NRETRD$=1$ → The Willenborg model is chosen.
NRETRD$>0(\neq 1)$→ The Vroman model is of concern.

In consideration of retardation, the plastic zone at the crack tip needs to be calculated with the aid of Eq.(16), that is,

$$R_{yoi}=\frac{1}{c\pi}\left(\frac{K_{maxoi}}{\sigma_y}\right)^2 \tag{40}$$

The coefficient c in the above equation differs according to the stress condition and hence this value is controlled by use of the control parameter NPLANE in the following fashion:

NPLANE=0 → This corresponds to the plane stress condition, and c is chose as $c=2$.
NPLANE≠0 → This is for the case of the plane strain condition, with c being put to be $c=4\sqrt{2}$.

3.3. Shape of crack and its location

Though the shape of the crack would vary widely according to the specimen geometries and loading conditions, the present program deals only with through-the-thickness crack, since this type of crack could be deemed to appear quite frequently in the practical applications.

The location of the crack is chosen by use of the control parameter NLOC as follows:

NLOC≧0 → This is the case for the through-the-thickness center crack.
NLOC<0 → This corresponds to the case of the through-the-thickness single edge crack.

3.4. Input data for random loading specifications

Assuming the case of aircraft structures, the input random load is treated in terms of the unit flight of necessary random loading cycles where a unit loading cycle consists of a pair of the minimum stress σ_{min} and the maximum stress σ_{max}. The load unit may be given by absolute unit in terms of kgf/mm^2 or by percentage of the design limit stress σ_{lim} (kgf/mm^2). In the latter case, conversion to the absolute unit is performed automatically inside the program. In other words, in case that σ' is prescribed by percentage unit of σ_{lim}, then the conversion

$$\sigma=\sigma'\cdot\sigma_{lim}/100.0(\text{kgf/mm}^2) \tag{41}$$

is made. This load unit is controlled by the parameter MSCON in the following way:

MSCON≧0 → The input load cycles are given by the absolute unit (in terms of kgf/mm^2).
MSCON<0 → The input load cycles are given by % σ_{lim} unit (unit is prescribed as % of σ_{lim}).

Since the present program never deals with negative stresses, the replaced value is applied in such a case that the minimum stress σ_{min} or the maximum stress σ_{max}, converted to absolute unit in terms of kgf/mm^2, assumes the following value. At that time, the original stress data are expressed "as prescribed" and the converted data "as modified".

$$\sigma_{min} < 0 \quad \rightarrow \sigma_{min} = 0 \text{ kgf/mm}^2$$
$$\sigma_{max} < 0.01 \rightarrow \sigma_{max} = 0.01 \text{ kgf/mm}^2$$

Further, dealing with the design limit stress σ_{min}, the function to quit computation is supplied when the design limit stress intensity factor, K_{lim}, exceeds the fracture toughness K_{IC} or the material of interest. K_{lim} is calculated under the assumption that specimen with the present crack length a is uniformly loaded with σ_{lim} as

$$\begin{aligned} &K_{lim} = \sigma_{lim} \cdot F(a) \\ &F(a) = \text{the function to compute stress intensity factor} \end{aligned} \tag{42}$$

In the case that no consideration is made of this design limit stress which is utilized widely for aircraft design and so forth, the parameter SIGLIM is prescribed as follows:

SIGLIM=0.0

In addition, since the input data are the history of random loading per unit flight, the statistical properties can be investigated by obtaining the mean with respect to the power exponent. In case of POWER=2.0, the root mean square value of the load-time history is computed.

3.5 Integration calculus of crack growth

Since the Paris-Erdogan's or the Walker's law is provided as the differential equation, the crack growth can be obtained by integrating this equation by cycle by cycle for each loading cycle. The integration is performed with the aid of area summing-up method in terms of sufficiently small divisions. However, it can be easily predicted that this method might lose cost performance in case of long fracture life, since the whole calculation consumes really a long time, although depending on the smallness of the divisions for integration. Therefore, the present program adopts the following way of computation:

Suppose that the current crack length is a and n times of loading cycles of $\sigma_{min} - \sigma_{max}$ are loaded. In case of $n=1$, the integration comes to be performed by cycle by cycle.

(i) First, ΔK and R or ΔK_{eff} and R_{eff} are calculated by use of the applied stresses σ_{min} and σ_{max} under the selected conditions. Then, da/dn is computed through the crack growth law of concern. At this time, in reference to the experimental results that both the crack growth rate and the retardation are not influenced strongly by the sufficiently small change in the crack length, the above calculation is carried out for the following expected value of crack length, with the sufficiently small change in crack length being $\Delta a = 0.01a$:

```
INPUT DATA FORMAT SAMPLE CHART -- PROBLEM IDENTIFICATION UP TO 80 CHARACTERS
SIGMAY    CKIC       DELKTH    EXPM       EXPN       CONST(E12.5)RCUT
HALFW     T             NLOCHRETRD NTYPENPLANE NCASE
C0(I),I=1,NCASE --- FORMAT(10F8.5)
 NLOADPOWER      SIGLIM      MSCON
SGMIN(I),SGMAX(I),I=1,NLOAD --- FORMAT(10F8.3) --- MIN. AND MAX. STRESSES.

----- SAMPLE INPUT DATA FORMAT -----
CASE-2: WALKER'S EQUATION; WILLENBORG' MODEL; CENTER CRACK; C0=3.0MM
50.0      68.0      2.5       0.31000   3.400     1.7500   -090.500
10.0      2.0                 1       1       1       1       1
3.0
   502.0       20.0              1
0.00    4.00    1.60    7.60    2.80    6.00    4.60    7.40    2.80    7.40
2.00    7.60    2.00    5.60    1.40    6.20    2.80    6.60    3.40    7.00
1.20    5.80    3.00    7.20    2.00    5.40    3.00    7.60    8.40    6.20
3.60    5.20    2.00    5.40    4.00    7.20    2.80    6.00     .80   10.60
2.60    5.40    2.80    7.20    3.40    7.80    1.80   10.40    3.00    4.80
1.80    6.80    4.80    8.00    2.00    4.00    2.60    3.80    1.80    4.60
2.60    9.20    3.60    6.20    2.20    4.60    2.20    3.60    1.60    7.80
5.00    8.60    3.00    7.40    4.40    7.60    4.60    7.60    2.80    5.00
3.00    6.40    1.80    7.40    5.80   11.80    2.60    5.80    2.20    5.60
2.80    8.60    3.00    4.80    1.60    6.60    2.20    7.60    1.80    6.60
```

Fig. 7 Input data format.

$$a=a+\frac{1}{2}\Delta=1.005a$$

(ii) Compare $\Delta a/(\frac{da}{dn})$ with a given number of cycles n.

(a) In case that $\Delta a/(da/dn)>n$, the crack growth at this step is deemed as $(\Delta a)'=n\cdot(da/dn)$ and the next loading step is followed with the new crack length of $a=a+(\Delta a)'$.

(b) In case that $\Delta a/(da/dn)\leqq n$, the crack length and the number of cycles are modified as follows:

$$\left.\begin{array}{l} a=a+0.01a \\ n=n-0.01a/(da/dn) \end{array}\right\}$$

Based upon the above conditions, this loading step is re-calculated through the preceding procedures.

(iii) When calculations are completed for all the input loading histories per one flight, the crack length at that time is stored into the memory. Then, the same computation is performed for the next flight, returning to the first step (i).

(iv) Fracture or failure is assumed when the larger value of either K_{llm} for the design limit load or K_{max} for the maximum spectrum load exceeds K_{IC}. Further, in order to examine the effect of ΔK_{th}, by comparing ΔK_{eff} with ΔK_{th}, when ΔK_{eff} for the current loading cycle is not greater than ΔK_{th}, no computation of the crack growth is made and the next loading cycle is proceeded under the assumption that no crack grows. Therefore, the effect of the threshold stress intensity factor range is ignored in case of the input condition of $\Delta K_{\mathrm{th}}=0.0$.

3.6 Input data and their format

An example of the input data necessary for the calculation in the present program is represented in Fig. 7. The data on one line in the figure correspond to one card in case of card input system. The brief explanation is given in what follows. It should be mentioned that the parentheses ( ) behind a variable shows the format for the present computer program, which can be easily modified as the occasion may demand.

(i) The first card (the first line in Fig. 7)
IDENT(40A2) = This is supplied to identify the case of computation. This can be given up to 80 characters in the present example, and may be easily modified according to the occasion.

(ii) The second card (the second line in Fig. 7)
SIGMAY(F10.5) = the yield stress of the material, σ_y [kgf/mm²]
CKIC(F10.5) = the fracture toughness, K_{IC} [kgf/mm² $\sqrt{\mathrm{mm}}$]
DELKTH(F10.5) = the threshold stress intensity factor range, ΔK_{th} [kgf/mm² $\sqrt{\mathrm{mm}}$]
EXPN(F10.5) = the power exponent v in the Walker's law. In case of applying the Paris-Erdogan's law, this value is regarded as dummy.
EXPM(F10.5) = the power exponent m in the Walker's or the Paris-Erdogan's law.
CONST(E12.5) = the constant value C in the Walker's or the Paris-Erdogan's law.
RCUT(F10.5) = the upper cut-off stress ratio, R_{cut}.

(iii) The third card (the third line in Fig. 7)
HALFW(F10.5) = the half width of the specimen, $w/2$ [mm]
T(F10.5) = the thickness of the specimen, t [mm]
NLOC(16) = the identification parameter for the crack location
NLOC $\geqq 0 \rightarrow$ the center crack
NLOC $< 0 \rightarrow$ the single edge crack
NRETRD(16) = the selection parameter of the retardation model
NRETRD $\leqq 0 \rightarrow$ to neglect retardation
NRETRD $= 1 \rightarrow$ the Willenborg's model
NRETRD $> 0 (\neq 1) \rightarrow$ the Vroman's model

NTYPE(I6) = the selection parameter of the crack growth law
NTYPE = 0 → the Paris-Erdogan's law
NTYPE ≠ 0 → the Walker's law

NPLANE(I6) = the stress condition parameter for the calculation of the plastic zone at the crack tip
NPLANE = 0 → the plane stress condition
NPLANE ≠ 0 → the plane strain condition

NCASE(I6) = the number of different initial crack length in predicting life for various initial crack lengths under the same stress (loading) condition

(iv) The fourth card (the fourth line in Fig. 7)

CO(I), I = 1, NCASE···Up to NCASE can be used for different initial crack length (10F8.5). In case that NCASE is larger than 10, the fifth card is also used with the same FORMAT.

(v) The fifth card (the fifth line in Fig. 7)

NLOAD(I6) = the number of loading cycles per one flight

POWER(F10.5) = the power exponent for mean square of loads. In case of POWER = 2, the root mean square (rms) value of the applied stress history can be obtained.

SIGLIM(F10.5) = the design limit stress, σ_{lim} [kgf/mm^2].
In case of disregarding this, SIGLIM = 0.0

MSCON(I6) = the identification parameter for the unit of loading histories per one flight
MSCON ≧ 0 → The unit is given in terms of kgf/mm^2
MSCON < 1 → The unit is given in terms of % of the design limit stress, σ_{lim} [kgf/mm^2].

(vi) After the sixth card (the sixth line in Fig. 7)

NLOAD number of loading histories are provided as a pair of σ_{min} (SIGMIN(I)) and σ_{max} (SIGMAX(I))(10F8.3). Since one card has 5 pairs of σ_{min} and σ_{max}, (that is 5 loading cycles), the corresponding number of cards needs to be given in order to supply the given number of loading cycles per one flight.

4. Numerical Computations and Discussions

4.1 Simulated results of crack propagation life

Though it is of much interest to compare the simulated results with actual experimental data, unfortunately at this time, there have been no available experimental data so far. Therefore, in the present study, such virtual data as shown in Fig. 7 as "SAMPLE INPUT DATA FORMAT" are applied for the crack growth prediction by use of this program. The parameter values adopted for this computation are given, assuming those for aluminum alloy, as follows:

$\sigma_y = 50$ kgf/mm^2
$K_{Ic} = 68$ kgf/mm$^2\sqrt{\text{mm}}$
$K_{th} = 2.5$ kgf/mm$^2\sqrt{\text{mm}}$
$v = 0.310$
$m = 3.40$
$C = 1.750 \times 10^{-9}$
$R_{cut} = 0.5$
$w/2 = 10.0$ mm
$t = 2.0$ mm

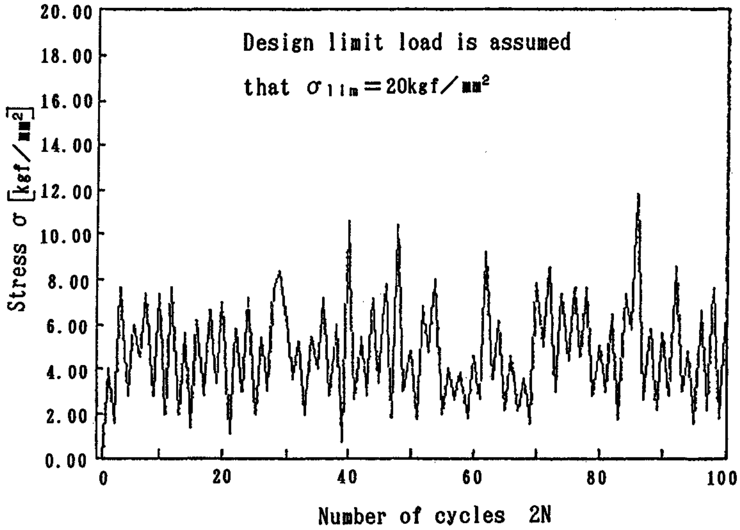

Fig. 8 An example of gust loading histories.

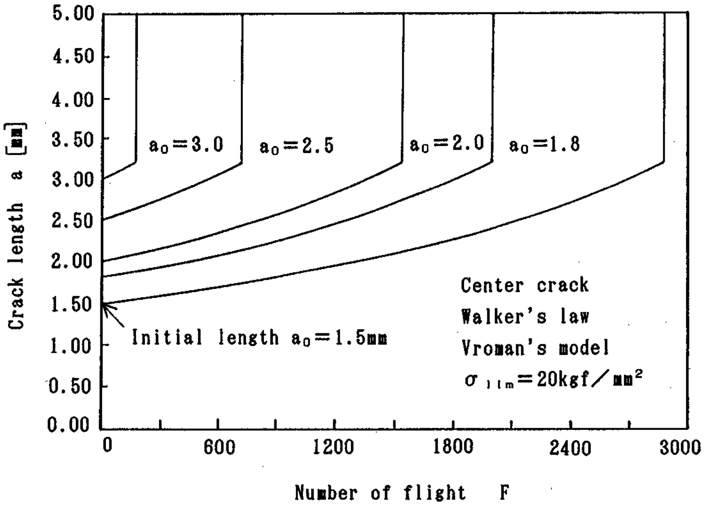

Fig. 9 Simulated results of the fatigue crack growth.

$\sigma_{\mathrm{llm}} = 20\ \mathrm{kgf/mm^2}$

As random loading histories for the input data, such loading histories as indicated in Fig. 8 are applied, which were obtained by the simulation of the gust loads subjected to the flight vehicle. Loading cycles in one flight are assumed for 100/2= 50 cycles.

The maximum value of the loading history is supposed to be around 60% of the design limit stress of $\sigma_{\mathrm{llm}} = 20\ \mathrm{kgf/mm^2}$.

Figure 9 represents the simulated results with the aid of both the Walker's crack growth law and the Vroman's retardation model. In this case, the initial crack length assumes 5 different kinds of values such as

$a_0 = 1.5,\ 1.8,\ 2.0,\ 2.5$ and $3.0\ \mathrm{mm}$

From this figure, the crack growth proves to cease when the crack length becomes around 3.2 mm, which satisfies the fracture condition such that $K_{\mathrm{llm}} \geqq K_{\mathrm{IC}}$ since the design limit stress σ_{llm} is set to be $20\ \mathrm{kgf/mm^2}$.

4.2. Effect of design limit stress

Next, in order to examine the effect of the design limit stress, σ_{llm}, such a case is simulated as $\sigma_{\mathrm{llm}} = 0.0\ \mathrm{kgf/mm^2}$ and the initial crack length $a_0 = 3.0\ \mathrm{mm}$. As can be clearly seen in Fig. 10, the crack is observed to propagate to more than 6 mm in length until fracture takes place. This fact may be an evidence for the satisfactory processing of the present program.

4.3 Comparison between Paris-Erdogan's and Walker's growth law

Figure 11 represents the difference in simulated results between the Paris-

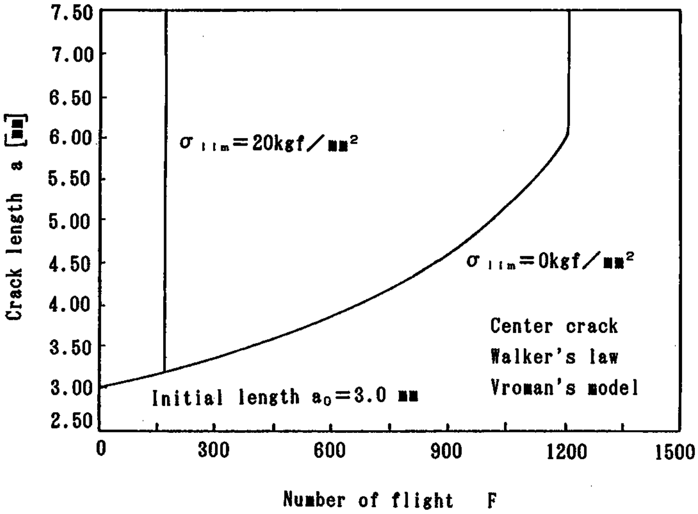

Fig. 10 Effect of design limit stress σ_{llm}.

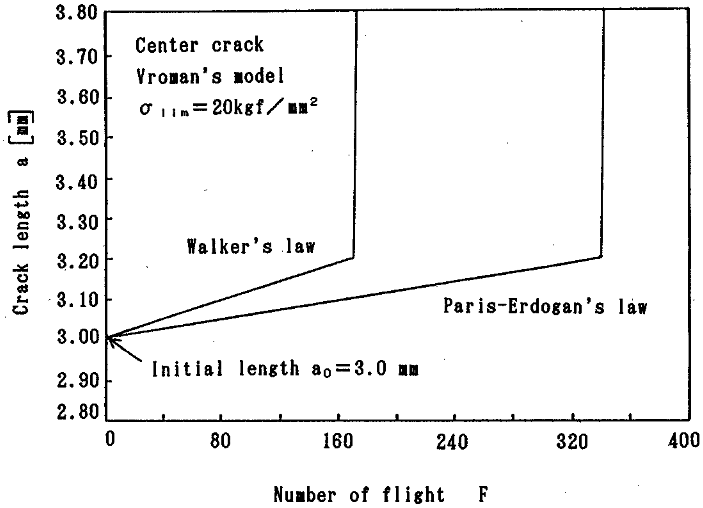

Fig. 11 Comparison between Paris-Erdogan's law and Walker's law.

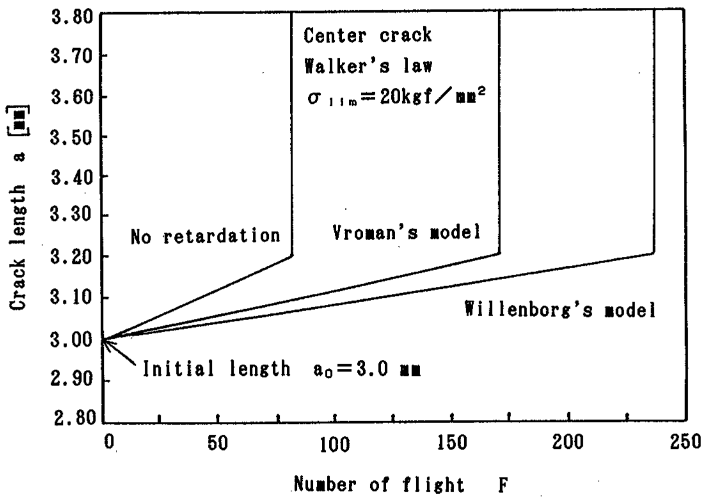

Fig. 12 Comparison between two retardation models.

Erdogan's law and the Walker's law. Such great difference as can be seen in this figure may be due to the situation that the material constants m and C are prescribed as really the same in both equations.

4.4. Comparison of retardation models

Figure 12 provides the effect of the retardation model on the simulated results. In case of ignoring retardation, fatigue life is simulated to be shorter, that is, to a safer side. On the other hand, in consideration of retardation, the Willenborg's model brings less safe results that the predicted life becomes longer than that by the

Vroman's model. Therefore, the Vroman's model may be considered more desirable than the Willenborg's model in a practical sense.

As can be clearly observed from the above figures, the validity and applicability of the present simulation program can be fully clarified.

5. Concluding Remarks

The present study develops the simulation program for the estimation of fatigue life under random loading in consideration of the retardation effect, which undoubtedly plays a crucial role in the reliability-based fatigue-proof design. With the aid of the program, the retardation effect can be clarified for given random loading cycles. The present program is applicable to various practical engineering problems associated with crack propagation. With respect to the applicability of this program, brief suggestions for future study are provided as follows:

(1) In such complex structures as aircraft and so forth, the shape of fatigue crack to exist or to be initiated would vary widely and the loading conditions also have a wide variety. Even for those cases, the present program can be easily extended and modified as the occasion may demand. More specifically, it would be easy to modify the present program to the case of crack shapes other than through-the-thickness center and single edge, or the case of cracks which propagate from rivet holes.

(2) By integrating the following crack growth law,

$$da/dn=f(\Delta K,\ R,\ \cdots)$$

the crack growth curve and the fatigue life are obtained. It is often the case that the calculation of the integration process is time-consuming and considerably costly. Hence, it is of practical importance to study the method to shorten execution time of the present program, for example, by transforming this differential equation to the equation which can be directly integrated with the aid of polynomial approximation. This method will enable many cases to be simulated in a short time, and also enables reliability analysis by use of Monte Carlo simulation technique.

(3) Since gust loads and so forth can be treated as stationary random processes, the simulation for such loads can be performed comparatively easily. On the other hand, flight loads are considered non-stationary random processes in the light of their nature. Consequently, from the practical viewpoint, it would be of vital significance to construct the simulation method for random loading as a non-stationary random process[14).

(4) By the repetition of varying loads, fatigue damage is accumulated gradually and fracture takes place finally through the initiation and propagation of cracks. The residual strength might decrease according to the crack growth. Hence, it becomes of much importance to clarify the probabilistic nature of the residual strength and to develop the method for analyzing structural reliability in relation to random loading.

References

1) P.C. Paris, and F. Erdogan, A Critical Analysis of Crack Propagation Laws, J. Basic Eng., Trans. ASME, **85**, 528-533 (1963).
2) R.G. Forman, V.E. Keamey and R.M. Engle, Numerical Analysis of Crack Propagation in Cyclic-Loaded Structures, J. Basic Eng., Trans. ASME, **89D**, 459 (1967).
3) J.E. Collipriest and R.M. Ehret, Computer Modeling of Part-Through-Crack Growth, SD 72-CE-15, Rockwell International, Space Division (1972).
4) K. Walker, The Effect of Stress Ratio during Crack Propagation and Fatigue for 2024-T3 and 7075-T6 Aluminum, ASTM STP, **462**, 1-14 (1970).
5) L.R. Hall, R.C. Shah and W.L. Engstrom, Fracture and Fatigue Crack Growth Behavior of Surface Flaws and Flaws Originating at Fastener Holes, AFFDL-TR-74-47, Air Force Flight Dynamics Laboratory, WPAFB, Ohio (1974).
6) P.D. Bell and M. Creager, Crack Growth Analysis for Arbitrary Spectrum Loading, AFFDL-TR-74-129, Air Force Flight Dynamics Laboratory, WPAFB, Ohio (1974).
7) W. Elber, The Significance of Fatigue Crack Closure, Damage Tolerance in Aircraft Structures, ASTM STP, **486**, ASTM (1971).
8) J. Willenborg, R.M. Engle and H.A. Wood, A Crack Growth Retardation Model Using an Effective Stress Concept, AFFDL-TM-71 IFBR, WPAFB, Ohio (1971).
9) O.E. Wheeler, Crack Propagation under Spectrum Loading, FZM5602, General Dynamics, Fort Worth Division (1970).
10) E.P. Probst and B.M. Hillberry, Fatigue Crack Delay and Arrest Due to Single Peak Tensile Overloads, AIAA Paper No. 73-325, presented at AIAA Dynamic Specialists Conference, Williamsburg, Virginia U.S.A. (1973).
11) G. Vroman, Crack Propagation Analysis with Retardation, presented at ASTM E-24 Committee Meeting, Northrop Corporation, Hawthorne, California (1971).
12) H. Okamura, "Introduction of Linear Fracture Mechanics", p.105, Baifukkan (1976).
13) M. Ishida, "The Plastic Analysis of Crack and Stress Intensity Factor", p.160, Baifukkan (1976).
14) M. Shinozuka, Hiro. Ishikawa and H. Mitsuma, Data-Based Nonstationary Random Processes, Proceedings of Specialty Conference on Probabilistic Mechanics and Structural Reliability, Tucson, Arizona, U.S.A., pp.39-43, ASCE (1979).